

## Central European Journal of Chemistry

# Characterization of calcium carbonates used in wet flue gas desulphurization processes

### Research Article

Simion Dragan<sup>1</sup>, Alexandru Ozunu<sup>2\*</sup>

<sup>1</sup>Babeş-Bolyai University, Faculty of Chemistry and Chemical Engineering, 400028 Cluj- Napoca, Romania

<sup>2</sup>Babeş-Bolyai University, Faculty of Environmental Sciences and Engineering, 400294, Cluj-Napoca, Romania

#### Received 19 January 2012; Accepted 30 April 2012

Abstract: This paper presents an experimental characterization of two sources of calcium carbonate, limestone and calcium carbonate precipitate (CCP) used in wet flue gas desulphurization processes. Characterization of the two carbonate sources was carried out by chemical analysis, IR spectra, thermal behavior, particle size distribution for CCP, BET surface area and absorption capacity of SO<sub>2</sub> in calcium carbonate suspensions. The absorption temperature, suspension concentration and carbonate grain size were found to be the most influential parameters in the absorption capacity measurements.

**Keywords:** Calcium carbonate reactivity • Wet desulphurization • Absorption capacity • Calcium carbonate precipitate • Slurry concentration © Versita Sp. z o.o.

### 1. Introduction

Problems concerning environmental protection are extremely important nowadays, considering the large quantities of emissions ( $SO_2$ ,  $SO_3$ , HF, HCI, etc.) released into the atmosphere. A particular case is that of sulfur dioxide emanations. Sulfur dioxide is a harmful gas formed in large quantities by fuel combustion with air excess, which in the atmosphere transforms into sulfuric acid – a major component of acid rain, as sulfuric acid is extremely soluble in water.

Sulfur dioxide emissions into the atmosphere have increased with industrial development. Many countries have therefore adopted strict regulations regarding  $\mathrm{SO}_2$  emissions from fossil-fired boilers which represent one of the significant sources of  $\mathrm{SO}_2$  emissions. This pollutant has a large global impact and is associated with the environmental damages of acidifying rivers and lakes. The removal of  $\mathrm{SO}_2$  for various industrial sources was given a considerable attention during the last years. Many different methods for flue gas desulphurization (FGD) have been developed to reduce  $\mathrm{SO}_2$  emissions, including dry, semidry and wet processes [1,2].

The dominant procedures employed in desulphurization of exhaust gases are based on wet scrubbing, especially slurry scrubbing [3,4]. Absorption of  $SO_2$  into limestone, lime and dolomite slurry is the most frequently applied method due to its high degree of  $SO_2$  removal, low cost and widespread availability [4]. There are various factors that favor the use of lime, limestone and dolomite slurry in FGD processes:

- limestone and dolomite are abundant minerals and can be used in prepared slurries with absorbent properties;
- the specific properties of the aqueous slurries obtained by the partial dissolution of suspended particles with appropriate diameter, shape and composition facilitate an increase of the absorption rate;
- the product of SO<sub>2</sub> removal is gypsum, which is stable and reusable;
- the major disadvantage of this limestonegypsum desulphurization process concerns the calcium sulfate sludge.

Many researchers have studied sulfur dioxide absorption and mechanisms in different calcium carbonate suspensions [5-9].

# 2. Mechanism of SO<sub>2</sub> absorption in calcium carbonate suspension

In terms of chemistry and mechanism of  ${\rm SO_2}$  absorption in calcium carbonate suspensions, the literature agrees upon two main parts of the process which affect absorption: chemical absorption and dissolution of solid reagents.

Regarding the  $SO_2$  absorption mechanism into calcium carbonate suspensions, the following processes can be considered [5,6]:

1. – the transfer of SO<sub>2</sub> through the gas-film near the gas-liquid interface:

$$N_{SO2} = k_{g} (p_{SO2} - p_{SO2}^{*}) \tag{1}$$

where:  $k_g$  is the mass transfer coefficient at the gas side of the gas-liquid interface;  $p_{SO2}$  is the partial pressure of  $SO_2$  in the gas phase;  $p_{SO2}^*$  is the partial pressure of  $SO_2$  at the gas-liquid interface.

2. — the dissolution and diffusion of  $SO_2$  in the liquid phase:

$$SO_{2[g]} \leftrightarrow SO_{2[aq]}$$
-dissolution (2)

$$SO_{2[aa]} + H_2O \leftrightarrow H_2SO_3$$
 -hydrolysis of  $SO_2$  (3)

$$H_2SO_3 \leftrightarrow H^+ + HSO_3^-$$
-dissociation (4)

$$HSO_3^- \leftrightarrow H^+ + SO_3^{2-}$$
-dissociation (5)

3. - the dissolution of calcium carbonate particles:

$$CaCO_{3[s]} \leftrightarrow CaCO_{3[aa]}$$
 (6)

$$CaCO_{3[aa]} \leftrightarrow Ca^{2+} + CO_3^{2-}$$
 (7)

$$CO_3^{2-} + H^+ \leftrightarrow HCO_3^- \tag{8}$$

4. - the chemical reaction within the liquid phase:

$$SO_2 + H_2O + HCO_3^- \leftrightarrow HSO_3^- + CO_2 + H_2O$$
 (9)

$$SO_2 + H_2O + SO_3^{2-} \leftrightarrow 2HSO_3^{-}$$
 (10)

$$HSO_3^- + CO_3^{2-} \leftrightarrow SO_3^{2-} + HCO_3^-$$
 (11)

$$Ca^{2+} + SO_3^{2-} \leftrightarrow CaSO_3 \tag{12}$$

$$CaSO_3 + 0.5O_2 + 2H_2O \leftrightarrow CaSO_4 \cdot 2H_2O \tag{13}$$

The main factors influencing the dissolution of the calcium carbonate are the size and origin of the limestone, the pH of the liquid phase and the sulfite ion concentration in the suspension.

Smaller limestone particles dissolve faster and therefore have a higher yield SO<sub>2</sub> absorption rate. Higher sulfite ion concentrations in the suspension inhibit the dissolution process. This is a result of the sulfite crystallizing on the surface of the calcium carbonate. Temperature has a significant effect on the removal of the SO<sub>2</sub> which is more effective at lower temperatures.

Neglecting the desorption of sulfur dioxide (when the operation is carried out in a closed system or under a sulfur dioxide atmosphere) and water vaporization, the real process can be described by the simplified "characteristic equation" (Eq. 14) and global reaction s - I - g (Eq. 15):

$$\begin{aligned}
[CaCO_3 + A'']_s + [H_2SO_3 + SO_2 + H_2O]_l \to | \\
\to [Ca(HSO_3)_2 + H_2SO_3 + SO_2 + H_2O]_l + [CO_2]_s
\end{aligned} \tag{14}$$

$$CaCO_{3|_{1}} + 2H_{2}SO_{3|_{1}} = Ca(HSO_{3})_{2|_{1}} + CO_{2|_{1}} + H_{2}O_{|_{1}}$$
 (15)

where  $[\ ]_{s,l,g}$  represent the solid, liquid and gas phase, respectively.

The process structure can be represented as:

$$-T_{SO_2[l]_g} \longrightarrow -Dis_{SO_2} \longrightarrow -T_{H_2SO_3[l]_l} \longrightarrow -Ads \longrightarrow$$

$$-r.ch \longrightarrow Dis_{Ca(HSO_3)_a}$$

where:  $T_{SO2[]g}$  –transport of  $SO_2$  in the gas phase;  $Dis_{SO2}$  \_dissolution of  $SO_2$  in the liquid phase;  $T_{H2SO3}$  – transport of  $H_2SO_3$  in the liquid phase; Ads- adsorption of  $H_2SO_3$  on the calcium carbonates particles; r.ch- chemical reaction (15); Des-desorption of  $CO_2$  from liquid phase;  $T_{CO2}$  – transport of  $CO_2$  in the gas phase;  $Dis_{Ca(HSO3)2}$ -dissolution of  $Ca(HSO_3)_2$  in the liquid phase.

For the reaction between  ${\rm CaCO_3}$  particles and sulfurous acid there are three possible macro kinetic models:

- a) transfer of reactant through the fluid phase;
- b) transformation on the surface of solid granules;
- c) combined model of external transfer-transformation.

The flue gas desulphurization process is dependent on the solid used in the preparation of the absorbent suspension. It is very important to know how natural or synthetic materials can interact with sulfur dioxide dissolved in the suspension.

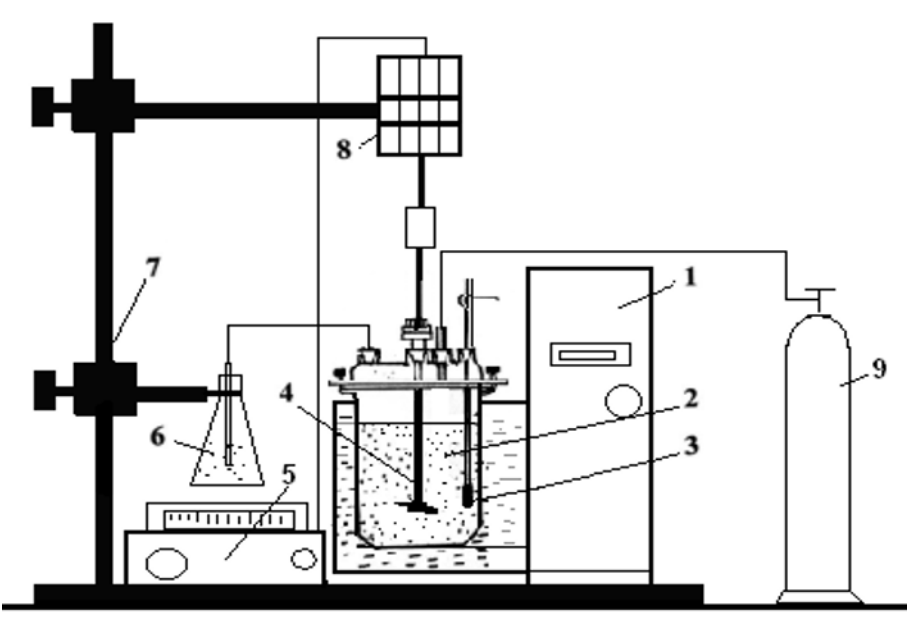


Figure 1. A schematic drawing of the experimental set-up: 1-Ultrathermostat, 2- reactor with stirring, 3-thermometer, 4-stirrer, 5-tachometer, 6-final gas neutralization vessel, 7-fixing support, 8-mixer motor, 9- sulfur dioxide cylinder.

# 3. Experimental procedure

The characterization of the two carbonate sources was carried out by crystallographic structure analysis. IR spectra were taken with a Digilab FTS 2000 spectrophotometer. Chemical reactivities were evaluated and analyzed by thermogravimetric measurements, using a TA Instruments SDT Q600 device at a heating rate of 10°C min-1. Limestone samples were crushed and sized on a Retsch set of sieves, with a mesh between 0-300 µm . Calcium carbonate precipitate (waste) was placed on the same set of sieves and sizing. The study of the sulfur dioxide chemisorption in the calcium carbonate slurry and the determination of the influence of temperature, particle size and suspension concentration on the absorption capacity of SO, in the two types of calcium carbonate slurries were achieved using the experimental equipment presented in Fig. 1.

The experimental set-up consists of a discontinuous 0.75 L reactor, fitted with a mechanical stirrer, a cylinder supply system for sulfur dioxide and final gas neutralization system.

To eliminate the possibility of the sulfur dioxide transfer through the gas phase becoming a rate-limiting step in the overall process development, experimental determinations were made with pure sulfur dioxide from a  $\mathrm{SO}_2$  bottle. Stirring of the suspension was adjusted so that the separating contact surface between the aqueous carbonate suspension and the gas phase was smooth, without waves generated by the moving slurry. The interface remained flat and steady. The unabsorbed gas was continuously exhausted and neutralized in the

hydroxide solution. The temperature was controlled using the ultra thermostat. The absorption experiments were performed at 298 K and 333 K at a constant rotation of the mechanical stirrer. The carbonate content of the suspension was 5, 10 and 20 g calcium carbonate / 100 g water, which corresponded to S/L ratios of 1/20; 1/10 and 1/5.

The evolution of the absorption process was measured using the iodometrical method based on the mass of the absorbed sulfur dioxide.

## 4. Results and discussion

The chemical compositions of the limestone and PCC were determined and are summarized in Table 1.

In order to determine the crystallographic structure and compare the two types of carbonates, crystallographic structure analysis was carried out. The IR spectra are shown in Fig. 1.

The IR spectra illustrated in Fig. 2 show that the two types of carbonates are not significantly different in terms of chemical and crystallographic structure. They exhibit the same maximum and minimum absorbance curve. Calcium carbonate precipitated in a wider band corresponding to a wavelength of 1450 cm<sup>-1</sup>. This can be attributed to the degree of crystallinity being lower than that derived from its rock. Chemical reactivity of the two varieties of calcium carbonates were evaluated and analyzed by thermogravimetric measurements, using a TA Instruments SDT Q600 device at a heating rate of 10°C min<sup>-1</sup>. The thermogravimetric analysis was

Table 1. Composition of limestone and calcium carbonate precipitate.

Carbonate source	Composition						
Limestone Sănduleşti - Turda	CaCO <sub>3</sub> [%]	Fe <sub>2</sub> O <sub>3</sub> [%]	Al <sub>2</sub> O <sub>3</sub> [%]	SiO <sub>2</sub> [%]			
	97.0	1.8	0.88	0.3			
Carbonate precipitate (waste) CCP	CaCO <sub>3</sub> [%]	Fe <sub>2</sub> O <sub>3</sub> [%]	NH <sub>4</sub> NO <sub>3</sub> [%]	humidity[%]			
	96.7	0.8	1.20	0.7			

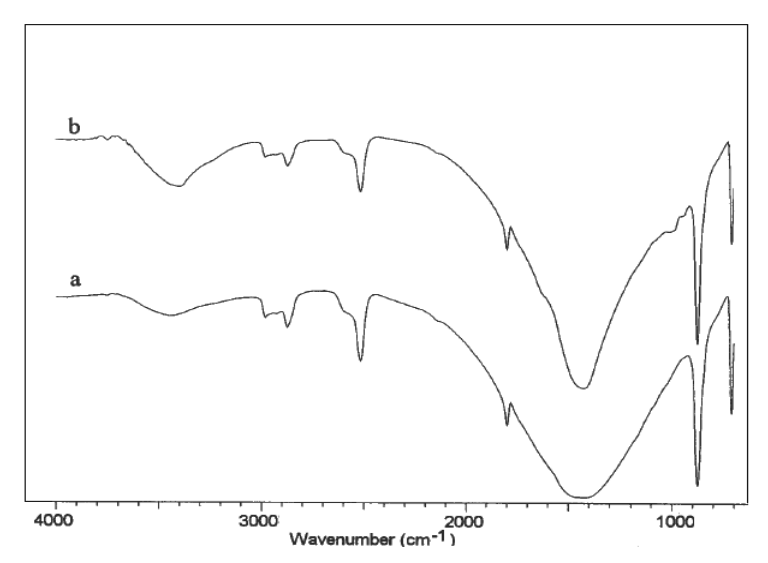


Figure 2. IR spectra of calcium carbonate. a.) - calcium carbonate precipitate (waste) of NP fertilizer industry; b) - natural limestone from Săndulești-Turda.

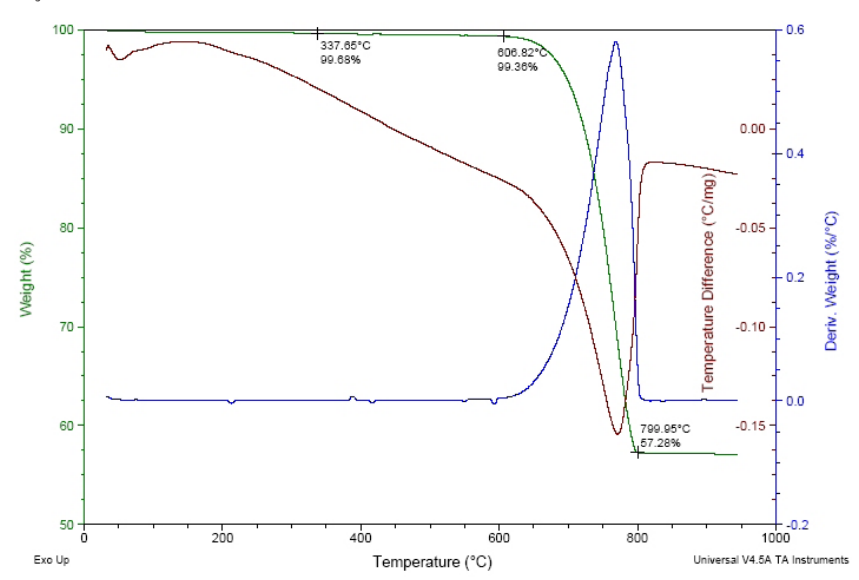


Figure 3. DSC-TGA for calcium carbonate precipitate (CCP).

performed, and the DSC-TGA curves recorded for the two types of carbonates are shown in Figs. 3 and 4.

A very similar behavior of the two types of carbonates can be observed, except the fact that the beginning of the dissociation temperature of CCP is 10°C lower than that of limestone (606.92 as compared to 617.69). Most significant are the differences between the corresponding

maximum decomposition velocity (DTG) which in the case of CCP is 740.5°C, whereas for limestone it is 777.02°C. These differences in temperature occurring during the thermal dissociation of the two varieties show a slightly higher reactivity of the PCC. Analysis of the thermograms shows that there are mass loss differences of 0.7% for CCP, respectively and 0.85% for limestone

in the temperature range in which these losses occur. These differences are justified by the presence of  ${\rm SiO}_2$  and  ${\rm Al}_2{\rm O}_3$  in the limestone, which are decomposed at higher temperatures. Limestone samples were crushed and sized on a Retsch set of sieves, with mesh sizes between 0-300  $\mu{\rm m}$ . Calcium carbonate precipitated (waste, CCP) was placed on the same set of sieves and sizing. The grain size distribution of CCP is shown in Table 2.

Sieve analysis results from Table 2 show that CCP particle size is less than 300 microns, while 60% of the

Table 2. The grain size distribution of CCP.

Mesh size sieve [mm]	Average size of the material [mm]	Mass fraction [g / g]	
0.200	0.255	0.098	
0.160	0.180	0.169	
0.100	0.130	0.136	
0.090	0.095	0.302	
0.080	0.085	0.105	
0.063	0.071	0.092	
0.056	0.595	0030?	
0.050	0.053	0025?	
0	0.025	0.042	

Table 3. Specific surface area of limestone and CCP.

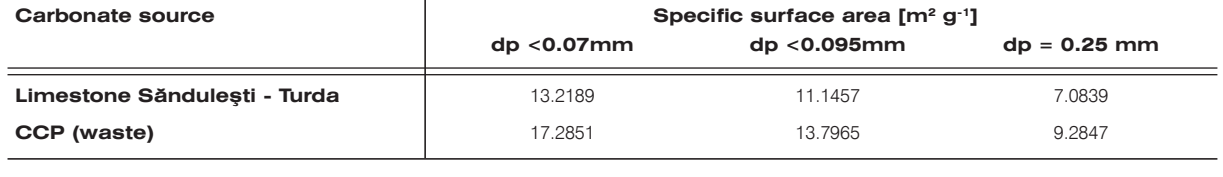
granule mass is associated with particles that have a diameter less than 95 microns. It should be mentioned that the fraction of particles between 200-300 microns represents only 9.8% of the total mass. These particle size classes used in the preparation of the slurry were characterized by BET surface area. For the two types of carbonates, these values are shown in Table 3.

The specific surface area of the CCP is greater than that of limestone for all three particle sizes examined, with values ranging between 17.74% and 23.7%. This is explained by the higher porosity of CCP particles compared to the limestone particles, especially with increasing solid grain size.

Porosity of the solid material plays a decisive role in the evolution of solid-fluid processes; these can change through the global rate of the process, due to the increase of the reaction surface.

The evolution of the absorption process was determined by the iodometrical titration method, measuring the amount of sulfur dioxide absorbed in water and in the two types of calcium carbonate slurries. Experimental kinetic curves obtained in sulfur dioxide absorption are shown in Figs. 5-9.

Solid grain size is one of the parameters significantly influencing the final absorption capacity, an aspect highlighted by the experimental results shown in



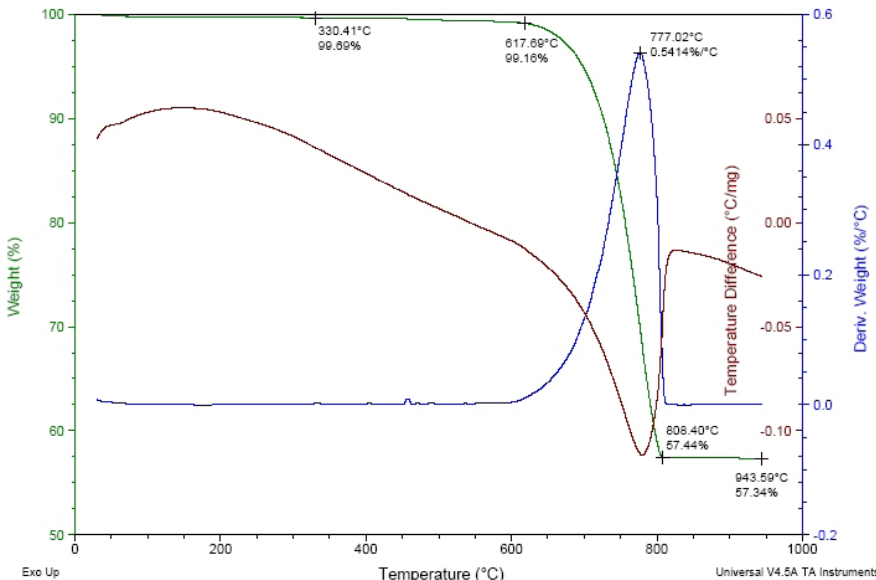


Figure 4. DSC-TGA for limestone

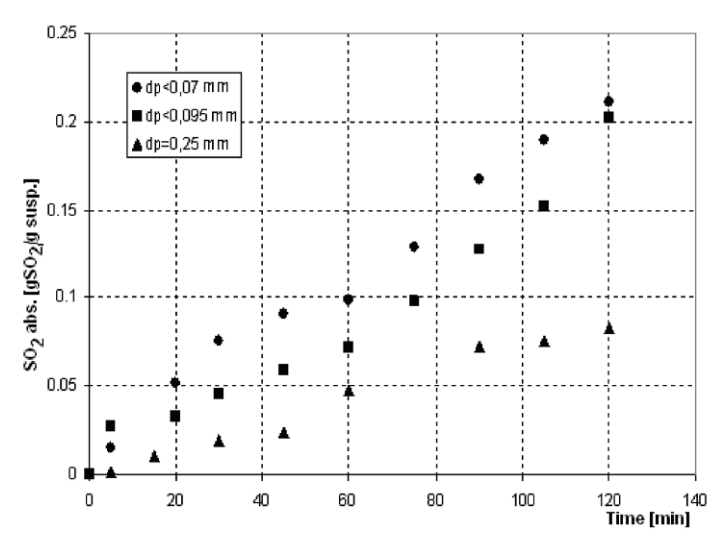


Figure 5. Kinetic data in sulfur dioxide absorption in CCP slurry with S/L=1/20 and T=298 K.

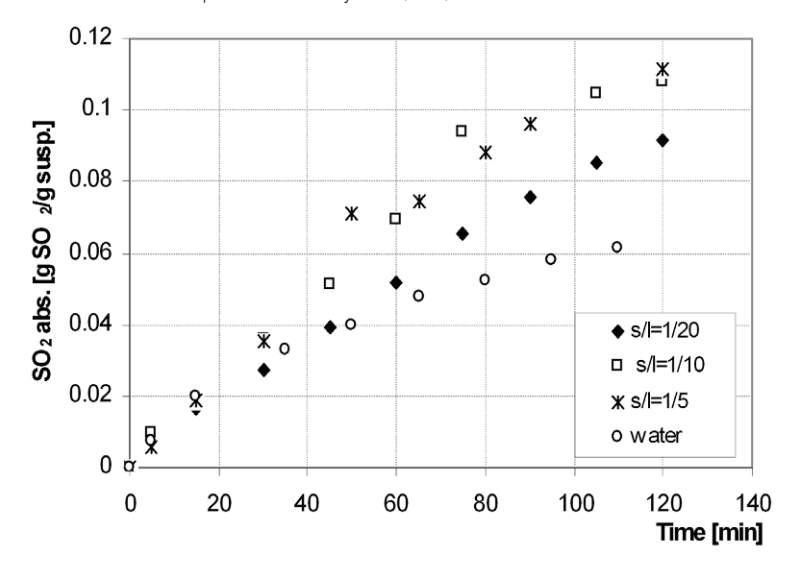


Figure 6. Kinetic data in sulfur dioxide absorption in limestone slurry with dp=0.25 mm and T=298 K.

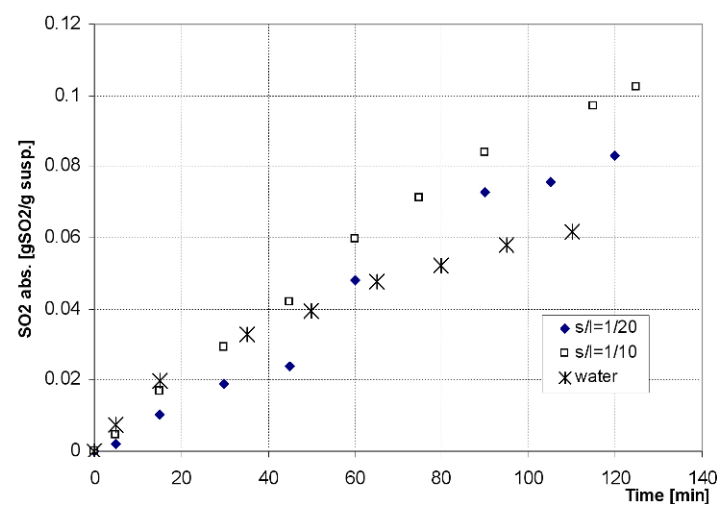


Figure 7. Kinetic data in sulfur dioxide absorption in CCP slurry with dp=0.25 mm and T=298 K.

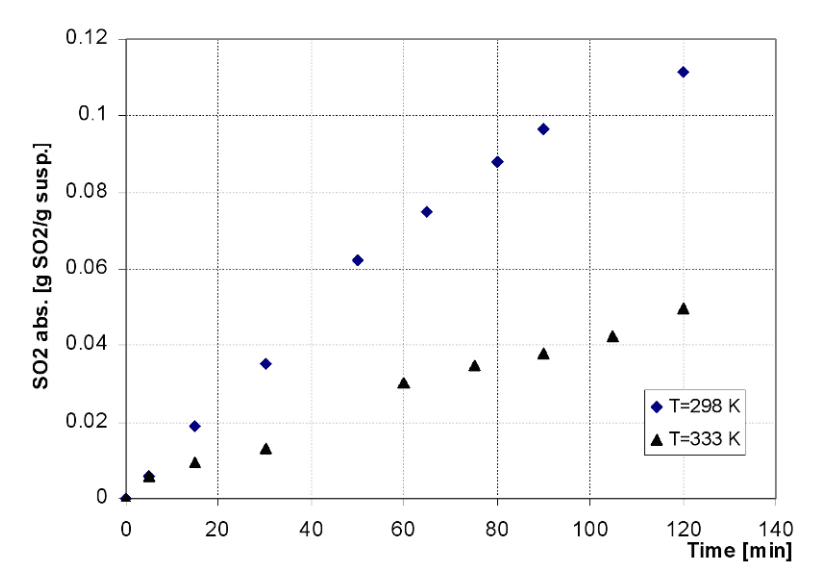


Figure 8. Kinetic data in sulfur dioxide absorption in limestone slurry with s/I=1/5 and dp=0.25 mm.

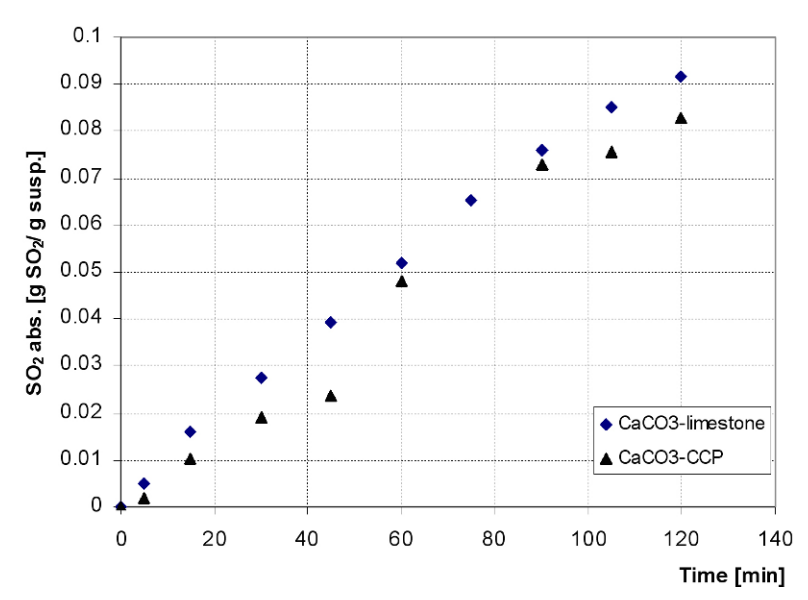


Figure 9. Kinetic data in sulfur dioxide absorption in calcium carbonate slurry with s/I=1/20, dp=0.25 mm and T=298 K.

Fig. 5. In the case of large grains, dp = 0.25 mm, it can be observed that at the beginning of the process, the absorption rate is very low and remains almost constant between 30-45 min. This is the stage of neutral calcium sulphite formation, which due to its extremely low solubility, determines the formation of crust on the surface of carbonate granules. When calcium bisulphite starts forming, it has a much higher solubility compared to the neutral sulphite, the crust is dissolved and the surface of the carbonate granules becomes accessible to  $SO_2$ , so that the absorption rate increases. As the concentration of calcium bisulphite in solution increases, the rate of its dissolution and absorption rate decreases.

If the particle size is smaller then the overall rate of absorption is higher, due to increased contact surface, which causes a faster dissolution of the reaction product. In Tables 4-6, experimental values obtained for the final absorption capacity of  $\mathrm{SO}_2$  in carbonate suspensions are presented.

As shown by the data presented in Figs. 5-9 and Tables 4-6, the final absorption capacity of  $SO_2$  varies a lot, depending on the temperature, the slurry concentration, the carbonate particle size and to a much lesser extent on the carbonate type. Thus, we obtained absorption capacities between 214 g  $SO_2$  / L slurry for the smallest particle size (dp <0.07 mm) in carbonate slurry with S/L = 1/10, to 83-92 g  $SO_2$  / L slurry, for the

Table 4. Influence of the solid grain on the final absorption capacity of SO2 in [g SO , / I suspension] at T = 298 K.

Absorbent Carbonate type	Water	Carbonate slurry with S / L = 1 / 20	Carbonate slurry with S / L = 1 / 10
Limestone with d <sub>p</sub> = 0.25 mm	62	92	115
CCP with d $_{p}$ = 0.25 mm	62	83	112
CCP with d $_{\rm p}$ < 0.095 mm	62	202	212
CCP with d $_{\rm p}$ < 0.07 mm	62	211	214

**Table 5.** Influence of temperature on the final absorption capacity of SO2 in [g SO <sub>2</sub> / I suspension].

Absorbent Carbonate type	т, к	Water	Carbonate slurry with S / L = 1 / 20	Carbonate slurry with S / L = 1 / 10	Carbonate slurry with S / L = 1 / 5
		62	92	115	116
Limestone : d <sub>p</sub> = 0.25 mm	298	62	91	113	-
	333	-	71	34	45
		-	70	33	-
Precipitated CaCO <sub>3</sub> : d <sub>p</sub> = 0.25 mm	298	62	83	112	117
		62	85	114	-
	333	-	78	62	46
		-	78	63	-

Table 6. Influence of carbonate slurry concentration on the final absorption capacity of SO2 in [g SO 2/1 suspension].

Absorbent Carbonate type	т, к	Water	Carbonate slurry with S / L = 1 / 20	Carbonate slurry with S / L = 1 / 10	Carbonate slurry with S / L = 1 / 5
Polydisperse limestone particles	298	62	86	115	117
	333	-	71	34	45
Polydisperse precipitated CaCO <sub>3</sub> particles:	298	62	83	110	120
	333	-	80	100	55

largest particle size (dp = 0, 25 mm) in carbonate slurry with S/L = 1/20. Absorbent suspensions with smaller particle sizes will have larger surface area because they have a greater surface area to volume ratio and therefore the absorbent will have a higher desulphurization capacity.

Another parameter that strongly influences the absorption capacity is the suspension consistency, as measured by the solid/liquid ratio (S/L). Experimental measurements of the absorption process were made at three different ratios: 1/20; 1/10; 1/5. With the increase of the consistency of the carbonate suspension to S/L = 1/20 and 1/10, the absorption capacity increases to

values of 200-214 g  ${\rm SO_2}$  /L slurry at a temperature of 298 K and grains with dp <0.07 mm. It is expected that the greater the consistency of the carbonate slurry, the greater its absorption capacity due to the formation of calcium bisulphite and calcium sulphite from the reaction. In fact, there was a decreased absorption capacity in the slurry with  ${\rm S/L}$  = 1/5 at 114-120 g  ${\rm SO_2}$  / L slurry, at the same temperature for both types of carbonates. This decrease of the final absorption capacity can be explained by an alternate macro kinetic mechanism that dominates the process. As the bisulphite solubility is limited, the sulphite-bisulphite crust produced by the reaction at the surface of the carbonates grains is so

compact that it prevents the penetration of  ${\rm SO_2}$  to the surface of the unreacted core of calcium carbonate granules.

Temperature significantly influences the final absorption capacity, but in a more complex way. With increased temperature, the solubility of  $SO_2$  in water decreases, and as a result, the absorption capacity decreases. Thus, at the high consistency of carbonate slurry, S/L=1 / 5, the final capacity of absorption is reduced from 117-120 g  $SO_2/L$  slurry, at a temperature of 298 K to values of 34-46 g  $SO_2/L$  slurry at a temperature of 333 K. The diluted suspension with S/L=1/20 shows that the capacity reduction is less significant: from 83-86 g  $SO_2/I$  suspension at 298 K, to 71-80 g  $SO_2/L$  suspension at 333 K.

The type of calcium carbonate has a minimum influence on the final absorption capacity. Regardless of slurry concentration, temperature or grain size, the differences between the final absorption capacities were of 2-5 g SO $_2$  / L slurry in favor of limestone. This is explained by the presence of impurities in limestone (Fe $_2$ O $_3$ , Al $_2$ O $_3$ , and SiO $_2$ ), which increase its reactivity towards SO $_2$ .

### References

- [1] H. Menig, Emissionsminderung und Recycling
   Grundlagen und Technologien (Ecomed Verlagsgesellschaft AG&Co. KG, Landsberg, 1996)
   (in German)
- [2] G. Astarita, D.W. Savage, A. Bisio, Gas Treating with Chemical Solvents (Wiley, New York, 1983)
- [3] S-M. Shih, J-P. Lin, G-Y. Shiau, J. Hazard. Mater. 79(1-2), 159 (2000)
- [4] SY. Liu, WD. Xiao, P. Liu, ZX Ye, Clean-Soil Air Water 36(5-6), 482 (2008)
- [5] P. Pellner, V. Khandl, Chem. Pap. 53(4), 238 (2002)

### 5. Conclusions

The chemical composition of the two types of carbonate is very similar as they both have CaCO3 contents higher than 96%. Thermogravimetric analysis shows a slight difference between the two types of carbonates. Thermograms show small differences between the beginning of the dissociation temperatures and temperatures at which the decomposition rate is at its maximum. IR analysis shows a very close equivalency between the two types of carbonates. Chemical reactivity is the main parameter that determines the use of the two types of carbonate in the flue gas desulphurization process. The influence of grain size on the overall process of SO, absorption in carbonate suspensions shows that the carbonate particle diameter used in the wet flue gas desulphurization must be less than 0.07 mm.

The experimental research shows that the waste calcium carbonate CCP from the NP fertilizer industry has a behavior similar to natural limestone and can be successfully used in the FGD processes.

- [6] R.V. Bravo, R.F. Camacho, V.M. Moya, L.A.I. Garcia, Chem. Eng. Sci. 57, 2047 (2002)
- [7] C. Hoşten, M. Gülsün, Min. Eng. 17(1), 97 (2004)
- [8] H. Gao, C. Li, G. Zeng, W. Zhang, L. Shi, S. Li, Y. Zeng, X. Fan, Q. Wen, X. Shu, Energ. Fuel. 24, 4944 (2010)
- [9] H. Gao, C. Li, G. Zeng, W. Zhang, L. Shi, S. Li, Y. Zeng, X. Fan, Q. Wen, X. Shu, Sep. Purif. Technol. 76, 253 (2011)